*Composites Part B* **29B** (1998) 819–827
1359-8368/98/$ - see front matter

PII: S1359-8368(98)00034-1

# Feasibility study of a passive smart self-healing cementitious composite

**Victor C. Li[a,*], Yun Mook Lim[b] and Yin-Wen Chan[c]**
[a]*Department of Civil and Environmental Engineering, University of Michigan, Ann Arbor, MI 48109-2125, USA*
[b]*Department of Civil Engineering, School of Civil and Urban Engineering, Yonsei University, Seoul (120-749), South Korea*
[c]*Department of Civil Engineering, Faculty of Engineering, National Taiwan University, Taipei, Taiwan, ROC*
*(Received 4 February 1998; accepted 20 April 1998)*

The basic concept of a passive smart-healing cementitious composite has been demonstrated, in the laboratory, to be feasible. The basic elements of this smart material include the sensors and actuators in the form of controlled microcracks and hollow glass fibers carrying air-curing chemicals. Controlled microcracking is offered by a strain-hardening engineered cementitious composite developed previously. The mechanisms of sensing and actuation are revealed through *in situ* environmental scanning electron microscopy observations. The self-healing effectiveness is confirmed by measurement of the elastic modulus of the composite. The elastic modulus is found to regain its original value in a repeat loading subsequent to damage in a first load cycle. © 1998 Elsevier Science Ltd. All rights reserved

**(Keywords: passive smart self-healing)**

## INTRODUCTION: PASSIVE SMARTNESS IN CIVIL INFRASTRUCTURES

Efforts in research and development of smart materials have been increasing rapidly in recent years (see, e.g., Ref. 1 for a broad overview). Most of these efforts have been directed towards high-performance, small-volume applications. For smart materials to be practical in civil infrastructures (CISs), several characteristics must be simultaneously satisfied. The smart material must be relatively low cost in a high material volume usage and cost-sensitive construction industry. The smartness is preferably self-actuated, with no external monitoring or human intervention. Finally, in CISs where structural members are large compared with components in most mechanical, electrical or biomedical devices, the smartness must be uniformly distributed and activated only when and where it is needed. In other words, a successful smart material in a practically realistic CIS application must be low cost, passive and distributed, in addition to being smart. These stringent requirements are generally difficult to satisfy.

In this article, an initial attempt to develop a Passive Smart Self-healing Engineered Cementitious Composite (PSS–ECC) for use in CISs is reported. The main function of the PSS–ECC is to seal and reheal cracks due to overloading, such as earthquakes. The objective is to maintain material and structural durability by regaining water tightness (sealing) and mechanical properties (healing) in concrete structures or building products based on cementitious materials. This is a feasibility study, with the focus on laboratory experimental demonstration of key concepts of the sensor and actuation mechanism. Data on recovered composite stiffness under repeated loading are also presented in a simplified version of this passive smart composite to verify the extent of self-healing.

In the following, the concept behind the PSS–ECC is explained in terms of its passiveness, distribution, sensor mechanism, actuation mechanism and self-healing ability. Next, the implementation of this concept into an ECC developed at the University of Michigan[2] is described. Finally, experimental confirmation of the sensing, actuation and self-healing effectiveness is presented.

## PASSIVE SMART SELF-HEALING CONCEPT

In a large-scale smart material, both the sensor and actuation mechanism must be ubiquitous and require no external monitoring or intervention. A simple method to achieve

* Corresponding author. Tel.: +1-734-764-4292; fax: +1-734-764-3368; e-mail: vcli@engin.umich.edu

such passivity and distribution is to build the sensors and actuators directly into the material characteristics themselves.

Cementitious materials are known to fail via tensile cracking when overloaded. Cementitious materials are extremely brittle, with tensile strain of about 0.01%, approximately one-tenth that of compressive strain, and with fracture toughness about 0.01 kJ/m$^2$ compared with 100 kJ/m$^2$ in mild steel. If the crack width is small and bridged by steel reinforcement, the structure may suffer from durability problems due to increased permeability of the concrete cover. The cracks provide enhanced pathways for aggressive agents to enter through the concrete cover and corrode steel reinforcement. If the crack width is large, tensile fracture and spalling may result, leading to a compromise in structural integrity. Even under overall compressive load, ultimate failure in cementitious material is preceded by local tensile cracking emanating from microdefects.

One self-healing concept is to release chemicals which seal the tensile cracks, followed by air curing of the released chemicals in the cracks, leading to regaining of mechanical properties of the uncracked composite[3]. In the present study, a Superglue (ethyl cyanoacrylate, a thermoplastic monomer manufactured by Loctite) serves as the sealing/healing chemical contained in hollow brittle glass fibers. Overloading is sensed by the brittle cementitious material by its innate brittleness. The resulting tensile cracking of the matrix and breaking of the glass fibers stimulate the actuating mechanisms in this totally passive smart material system. Once the glass fibers break, the chemical is released into the cracks of the cementitious matrix so that the cracks can be sealed and the composite rehealed. Hence, the cementitious matrix serves as the ubiquitous sensor, and the hollow glass fibers serve as the ubiquitous actuators.

Unfortunately, the self-healing mechanism described cannot work in normal concrete, cement or even fiber-reinforced concrete. This is because the width of the tensile cracks in such materials cannot be easily tuned. Localized fracture leads to continued increases in crack width under decreasing tensile load, and rapidly exhausts the amount of chemical available for crack sealing and composite rehealing. Thus, for the proposed self-healing concept to work, it is critical that the tensile crack width be controlled, and it must be limited to within tens of micrometers. Otherwise, very large hollow glass tubes will be needed, which in turn negatively modify the mechanical properties of the composite.

Apart from limiting the amount of chemical needed, the maximum allowable crack width is also limited by the effectiveness of the actuation mechanism. The actuation mechanism of releasing chemical into the matrix cracks is dependent on the capillarity of the thin channels created by the crack surfaces, against capillary force inside the hollow glass fibers resisting chemical release. Thus, the crack width of the matrix should be limited to less than the inner diameter of the glass fiber for effective actuation.

The ECC developed at the University of Michigan[2] has the normal constituents of fiber-reinforced mortar, including cement, water, sand and reinforcing fibers. Unlike normal fiber-reinforced concrete/mortar (FRC), however, ECC exhibits tensile strain-hardening characteristics. Under overload conditions, localized fracture does not form until a tensile strain of several percent is attained, significantly enhancing the margin of safety. Instead, damage associated with matrix microcracking occurs during strain-hardening, and the microcrack width can be controlled to within tens of micrometers or less, for overall tensile straining of less than 2%. A uniaxial stress–strain curve for an ECC is shown in *Figure 1*. For comparison, the stress–strain curve for a normal FRC is also included. For the latter, tension-softening begins at a tensile strain of about 0.03%, accompanied by a single, increasingly large crack width. For the specimen length used (200 mm) for the tension tests from which the stress–strain curves in *Figure 1a* were derived, the crack width for the FRC at 2% overall strain would be 4 mm. The unique characteristics of the ECC are a result of judicious choice of fiber, matrix and interface properties, made possible by the use of micromechanical principles[4,5]. *Figure 1b* illustrates the distributed damage behavior of an ECC. The width of the cracks shown is less than 0.1 mm.

The passive smart self-healing concept described above becomes feasible when combined with the strain-hardening

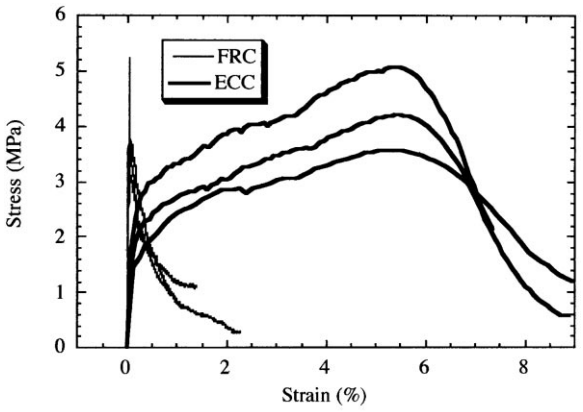


(a)

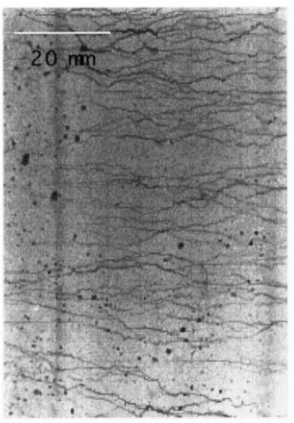


(b)

**Figure 1** (a) Uniaxial tensile stress–strain curves of an engineered cementitious composite (ECC) and an ordinary fiber-reinforced concrete (FRC). (b) Multiple cracking with fine crack width control in ECC (specimen shown has been tensile strained to 4.6%)

and crack-width control characteristics of the ECC. This is the basic concept behind the development of the PSS–ECC. In the following section, we describe some preliminary implementation and experimental observations to test the feasibility of the PSS–ECC concept.

## PASSIVE SMART SELF-HEALING CONCEPT: IMPLEMENTATION

### *PSS–ECC*

In the PSS–ECC system, sensing of overload is performed by the brittle cementitious matrix of an ECC material, while actuation of chemical release is performed by rupture of hollow glass fibers. The ECC material also serves to control crack widths.

To demonstrate the feasibility of the PSS–ECC concept, two different levels of experiments are designed and conducted. The first level involves model PSS–ECC material systems with a single hollow glass fiber without any sealing chemical, with the tests conducted *in situ* in a loading stage under an Environmental Scanning Electron Microscope (ESEM). The first-level experiments are designed for confirming the sensing and actuation mechanisms of the PSS–ECC in very small specimens, through direct observation under the ESEM. The second-level tests involve flexural specimens of PSS–ECC systems which contain glass fibers filled with sealing agent, named SAC fiber (Sealing Agent Carrying fiber). These experiments are conducted under standard (MTS) load frames and are intended to establish the rehealing effectiveness of the sealing agent after the material suffers crack damage in load cycles.

The material compositions of PSS–ECC specimens for the two-level tests are different (due to differences in fabrication needs of regular size and small size specimens for use in the ESEM) and are described in *Table 1*. For the ESEM test specimens, custom-made hollow glass fibers 500 $\mu$m in diameter and 60 $\mu$m in wall thickness are used. For the flexural beam experiments, commercial hollow glass fibers for medical application (micropipette for blood sampling) were adopted for convenience. The dimensions of the hollow glass fibers are 1.0 mm outer diameter, 0.8 mm inner diameter and 100 mm length, with 50 $\mu$l capacity. Superglue with fast air curing capability and low viscosity ( $<$ 5 cP) is selected as the sealing agent. To fill, a hollow glass fiber is held horizontally with one of the open ends placed into the sealing agent, which flows into the glass by capillary effect. After filling, both ends of the hollow glass fiber are sealed with silicone sealant to prevent the reaction of sealing agent with air or water. In this process, no air bubble is allowed in the SAC fibers.

Note that the ECCs contain Spectra (a high-modulus polyethylene) fiber intended as mechanical reinforcement for the cement matrix. The hollow glass fibers, however, are intended for carrying the sealing agent, and do not serve any reinforcing function.

### *Sensing and actuation mechanisms*

For the first-level test under the ESEM, the specimen shape and loading configuration are illustrated in *Figure 2*. For *in situ* wedge loading, two notches are created on both sides of the specimen. The specimen is prepared so that part of the hollow glass fiber is exposed on the surface for observation. Fiber orientation is varied in order to observe differences in fiber rupture mode at different inclination angles to approaching matrix cracks. The first-level test provides information on the interaction between the matrix crack in the ECC and the hollow glass fiber.

Wedges are driven into the notches, forcing them to open in a controlled manner. Cracks are initiated from the tips of the notches and propagated toward the glass fiber (*Figure 3*). These cracks may or may not join together, as shown in *Figure 3*. The matrix crack bridged by the glass fiber can

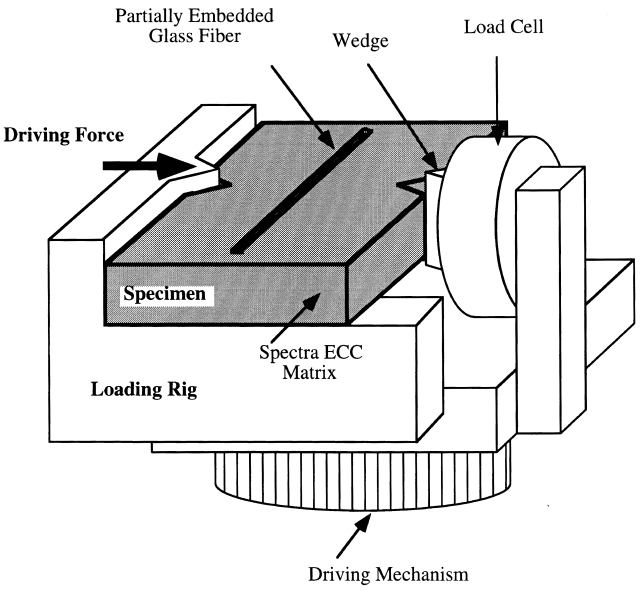


**Figure 2** ESEM specimen, loading stage and configuration. Specimen dimensions are 10 mm $\times$ 10 mm $\times$ 1.5 mm

**Table 1** ECC mix design

| Specimen | Cement | SF | SP | Water | Fiber ($V_f$) | Fiber |
|---|---|---|---|---|---|---|
| ESEM | 1.0 | – | – | 0.5 | 0.01 | Spectra* |
| Beam | 1.0 | 0.1 | 0.01 | 0.27 | 0.02 | Spectra† |

SF, silica fume; SP, Superplasticizer
*Spectra 900 with 38 $\mu$m diameter and 6.35 mm length
†Spectra 900 with 38 $\mu$m diameter and 12.7 mm length or Spectra 1000 with 28 $\mu$m diameter and 12.7 mm length

induce local debonding along the interface between the glass fiber and matrix. In *Figure 4*, separation between glass fiber and ECC material is clearly observed. As the matrix crack width increases, the debonded segment of the interface extends away from the matrix crack.

Breakage of the glass fiber was observed as the matrix crack opened to approximately 250 $\mu$m at the notch tip. Two different failure types were observed. *Figure 5a* shows glass fiber under direct tensile load, where the broken surface is straight and simple. In *Figure 5b*, the glass fiber breaks into fragments, showing a more complicated flexural failure. In general, the glass fiber tends to break in tensile mode for the cases of small inclined angles between glass fiber orientation and the longitudinal direction of specimen, whereas flexural failure is usually observed for large inclined angles.

To provide visual evidence of the actuation mechanism in this PSS–ECC system, the same ESEM *in situ* tests are performed with a glass fiber filled with red ink. The red ink is chosen for easy visual marking of the pathway of the released chemical. It has a viscosity approximately the same as the Superglue, which will serve as the actual sealing chemical. *Figure 6* shows three sequential stages of wedge loading, the corresponding matrix crack approach to a glass fiber, and flow of the red ink from the ruptured hollow glass fiber into the matrix crack and the debonded fiber/matrix interface.

These ESEM *in situ* experiments visually confirm that the sensing and actuation mechanisms are operative in the

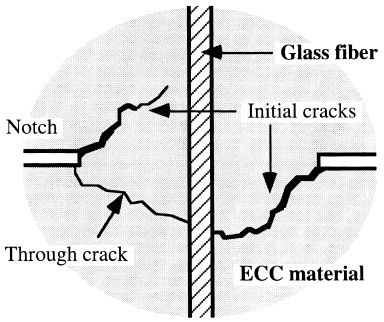


**Figure 3** Formation of through crack in ESEM specimens

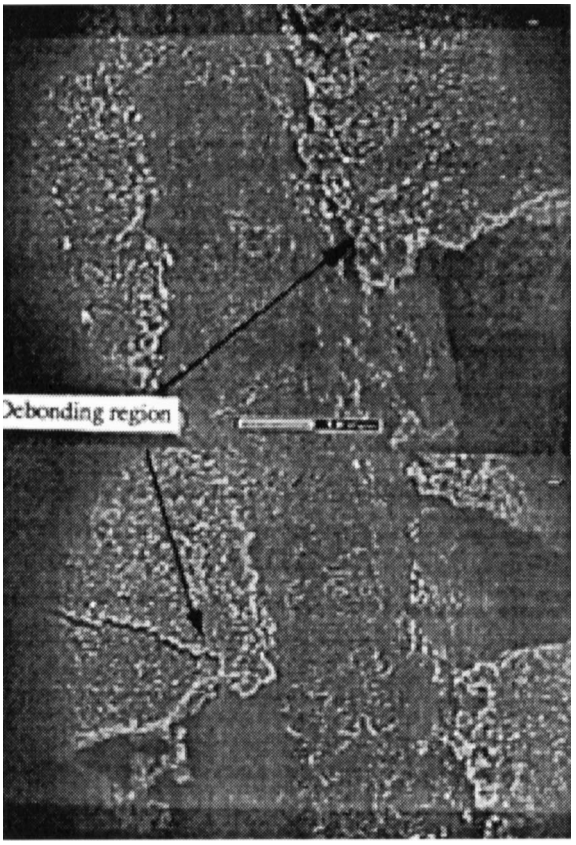


**Figure 4** Debonding region in the glass fiber/ECC interface

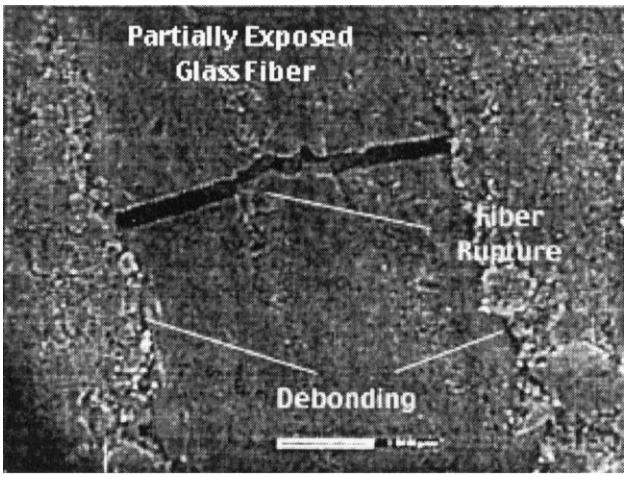


(a)

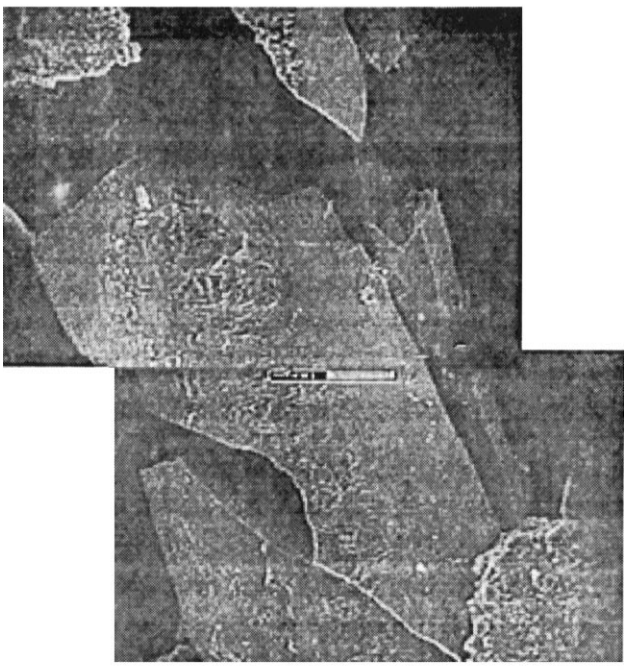

(b)

**Figure 5** Breakage shape of glass fiber: (a) simple breakage due to tensile load; (b) fragment breakage due to flexural load

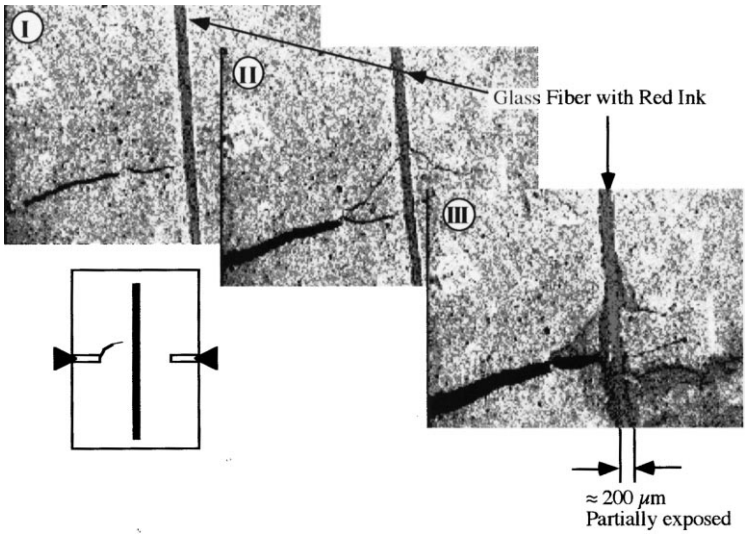


**Figure 6** Sequential view of actuation mechanism showing an ECC crack approaching a hollow glass fiber (I), interacting with a glass fiber (II), and glass

proposed PSS–ECC system. The glass fiber diameter, wall thickness and material brittleness, coupled with ECC matrix cracking, appear to be a suitable material system for the sensing action envisioned. Controlled crack width in the ECC and low viscosity of healing chemicals assist in easy release and sealing action of the healing chemicals in the ECC cracks, providing favorable conditions for an effective actuation mechanism.

## PASSIVE SMART SELF-HEALING ECC: EXPERIMENTAL CONFIRMATION

### *Flexural testing and specimens of model PSS–ECC*

The conceptual sensing and actuation mechanisms were implemented and visually confirmed in a model PSS–ECC material containing a single glass fiber, as described in the previous section. In this section, the self-healing mechanism of PSS–ECC is demonstrated by the regaining of material stiffness after damage is imposed by a mechanical load.

In this experiment, a three-point bending set-up is used under a close-loop MTS-810 machine with Test Star control system. *Figure 7* schematically illustrates the set-up of the test, specimen size and loading configuration. Nineteen specimens were cast and demolded after 24 h. They were then water cured at room temperature for 2 weeks. The specimens were dried for 24 h before testing. In addition, three specimens were cast in a different size (width 76.2 × height 101.6 × length 350.6, in mm), and tested under a four-point bending set-up (304.8 and 101.6 mm for span and center span length).

*Table 1* contains the mix proportion of the ECC composites. Two different types of fibers were used in this study. The M1 ECC contains Spectra 900 and the M2 ECC contains 1000 fibers. The differences in properties between materials M1 and M2 are ultimate strength and crack width. The average crack width was 50 $\mu$m in M1 and 30 $\mu$m in M2

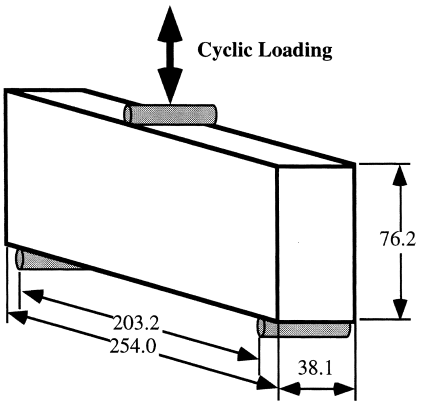


**Figure 7** Dimension of flexural specimen and loading configuration (units: mm)

at the unloading stage, and the ultimate flexural strength of M2 was about 10% higher than that of M1. The choice of these different ECCs in this study is mainly for convenience (fiber availability).

*Table 2* shows the different specimen types in terms of materials, number of SAC fibers and the dosage of sealing agent. The first letter of each specimen name indicates the presence or absence of SAC fibers: N (No. of SAC fibers), I (glass fibers with Ink instead of SAC fibers) and S (SAC fibers). The second letter refers to the fiber type (M1 or M2), and the last number '4' in some cases indicates the four-point bending test.

All PSS–ECC bending specimens specified in *Table 2* were loaded up to a pre-determined deflection of the beam beyond first cracking. At this stage, a certain amount of damage (in the form of visible micro-cracks) occurred on the tensile side of the specimens. The bending specimens were then immediately unloaded and rested for 5 min. This loading/unloading cycle was repeated once, followed by monotonic loading until specimen failure.

**Table 2** Specimens and dosage of sealing agent

| Specimens | No. of specimens | No. of SAC fibers | No. glass fiber w/ink | Amount of SA (ml) |
|---|---|---|---|---|
| N-M1 | 1 | – | – | – |
| N-M2 | 5 | – | – | – |
| N-M1-4 | 2 | – | – | – |
| I-M1 | 2 | – | 10 | – |
| S-M1 | 2 | 20 | – | 1.0 |
| S-M2 | 6 | 20 | – | 1.0 |
| S-M1-4 | 1 | 32* | 8* | 3.2 |

SA, sealing agent (Superglue)
*200 mm length and 100 $\mu$l capacity glass fibers with the same cross-section specified in the ''Passive Smart Self-healing Concept: Implementation'' section

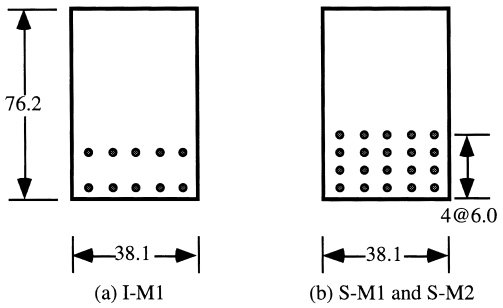


**Figure 8** Cross-section of flexural specimen, showing position of glass fibers (units: mm)

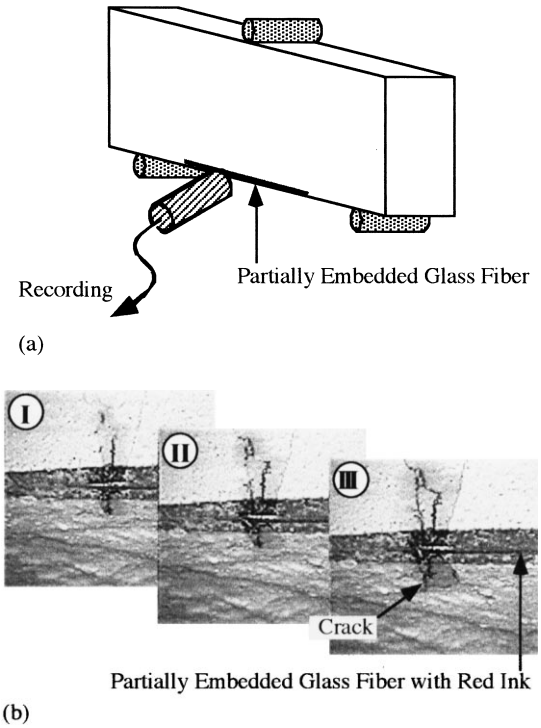


**Figure 9** (a) Red ink penetration observation technique. (b) Sequential pictures showing the actuation mechanism of red ink release

Displacement control was used for loading and force control was used for unloading; 0.2 kN was sustained for the healing period between unloading and reloading. An additional three specimens with M1 material were tested under monotonic loading as controls.

*Figure 8* illustrates the cross-section of S-M1, S-M2 and I-M1. The glass fibers were placed at the center of the specimens. For placing convenience, five SAC fibers in each layer were linked using a tape.

### *Experimental results*

The sensing and actuation mechanisms of the PSS–ECC beams were reconfirmed at the macroscopic level using the red ink penetration observation technique (*Figure 9a*). A single glass fiber filled with red ink was partially embedded at the edge of the tensile region in a specimen for external observation with the help of a $\times$ 20 magnification microscope during the test. *Figure 9b* shows the sequential release of red ink along cracks as flexural load increases, resulting in matrix cracking of the ECC, glass fiber rupture and red ink release. In addition, two PSS–ECC beams were tested with 10 red ink-filled glass fibers embedded in the interior of the specimen. Spots of red ink appeared on the surface of the specimen subsequent to flexural loading (*Figure 10*). This set of tests provides evidence of the sensing and actuation mechanisms under identical conditions for the SAC fibers embedded inside the ECC.

For evidence of the healing mechanism in PSS–ECC, the beam stiffness on repeated flexural loading is evaluated. If the healing mechanism is operative, regaining of stiffness is expected. Otherwise, micro-cracking caused by the first load cycle should lead to increased beam compliance.

It is important to recognize that regaining of load-carrying capacity in the PSS–ECC beams does not necessarily signify re-healing. For any material which does not lead to overall failure (macroscopic load-drop) after first cracking, but followed by strain-hardening accompanied by multiple cracking, the envelope for loading and reloading would follow the monotonic stress–strain (hardening) curve. Thus, further increase in load-carrying capacity in subsequent load cycles simply reflects the strain-hardening property of such materials, and cannot be used to confirm the operation of the healing mechanism. This statement holds for specimens loaded in flexure or tension, and applies to materials which achieve strain-hardening by whatever means (e.g., using fiber/wire mats as reinforcements), see e.g., Ref. 3.

Three beams were tested under monotonic loading conditions. *Figure 11* illustrates a typical load–deflection curve. The purpose of this monotonic loading test is to determine the first and second unloading points for the

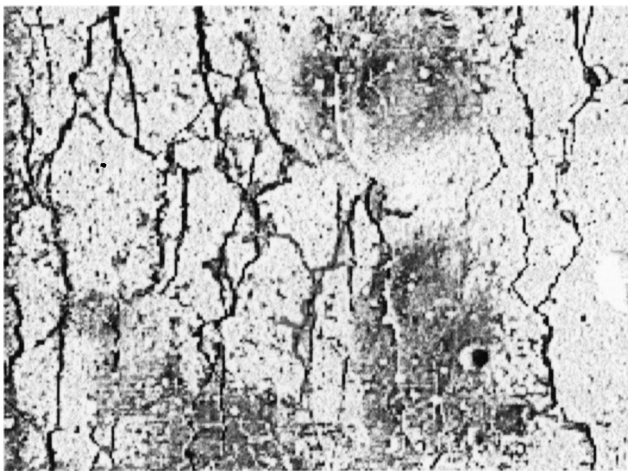

**Figure 10** Indirect evidence of sensing and actuation mechanisms showing red ink released from internally embedded ink-filled hollow glass fibers in flexural specimens

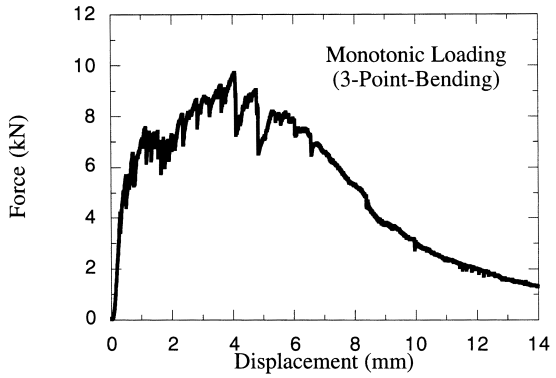


**Figure 11** Load–deflection curve in monotonic loading

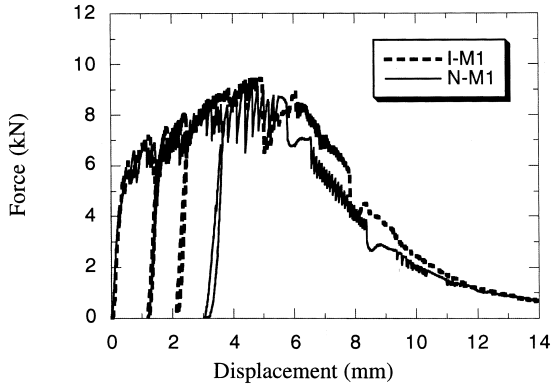


**Figure 12** Load–deflection curve in cyclic loading

cyclic loading, chosen to be in the strain-hardening region (beyond the first crack stress, but below the flexural strength). Beam deflections (1.5 and 2.5 mm) were selected for the first and second unloading points, respectively. In *Figure 12*, the results of cyclic loading without SAC fibers are illustrated. One (I-M1) has 10 glass fibers with red ink and the other (N-M1) has no glass fibers in the specimen.

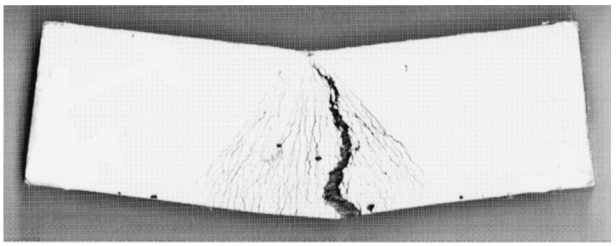

**Figure 13** Failure pattern of flexural specimens

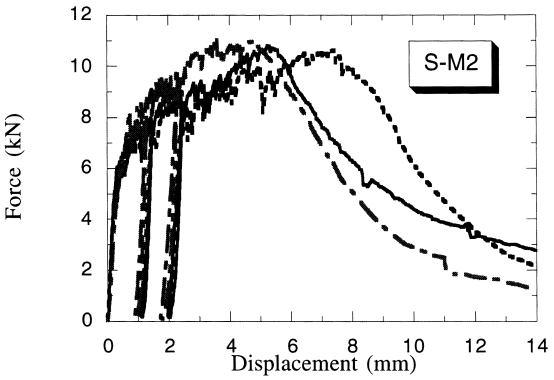


**Figure 14** Flexural test results in PSS–ECC materials

There is no significant effect on the load–deflection curve due to the presence of the glass fibers in these tests. The flexural failure pattern of the specimen is illustrated in *Figure 13*. The damaged zone is developed during strain-hardening of the ECC materials with intensive multiple crack development. This failure pattern occurred consistently for all test specimens.

In *Figure 14*, the load–deflection curves are illustrated for some S-M2 cases. These specimens contain SAC fibers. It is difficult to detect the stiffness changes in the macro load–deflection curve. For stiffness measurements, the linear portions of loading curves in enlarged data plots were used. To avoid initial sitting compliance of fixtures, data points between 2 and 3 kN were consistently used to calculate the stiffness. The upper limit was chosen to avoid material non-linearity associated with micro-cracks which initiate between 3.5 and 4 kN in the first load cycle. A linear curve fitting function was used to compute the stiffness. The mean and standard deviation of the coefficient of linearity are 0.990 and 0.0077, respectively.

The stiffness changes are reported in *Figures 15* and *16* for materials M1 and M2, respectively. Each stiffness is normalized by the initial stiffness (uncracked) of each specimen. Solid symbols represent PSS–ECC systems. Six out of nine specimens showed higher regained stiffness on first reloading than the initial stiffness, and two specimens were close to the initial stiffness. As a result, eight out of nine PSS–ECC specimens indicated recovery of stiffness. In contrast, specimens having no SAC fibers all suffered stiffness degradation from 10% to 40%.

For PSS–ECC specimens that did not perform as well, post-mortem investigations indicate hardened sealing agent inside SAC fibers. It seems that the sealing agent may have

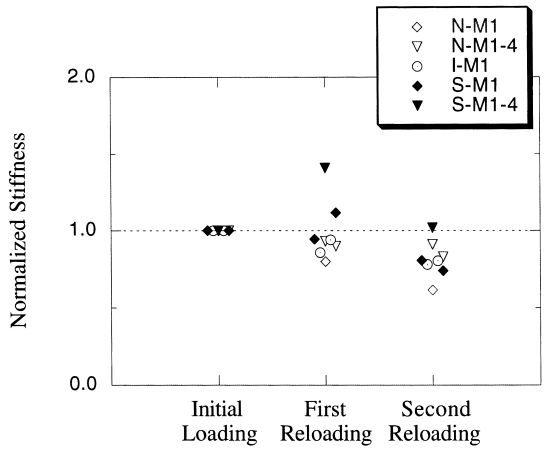


**Figure 15** Normalized stiffness in flexural beam with material M1

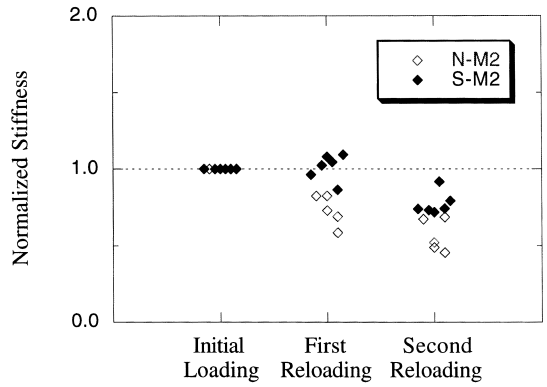


**Figure 16** Normalized stiffness in flexural beam with material M2

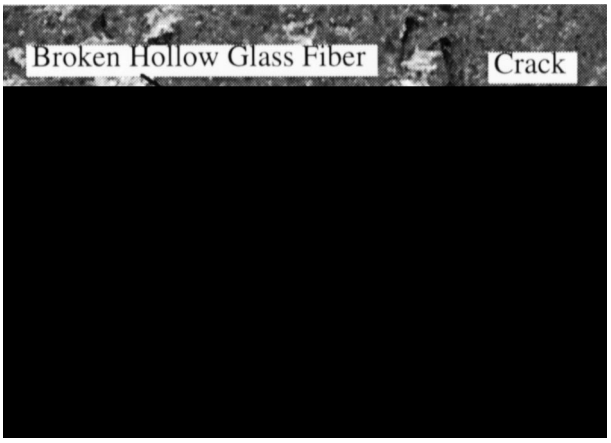


**Figure 17** Cut section of a specimen with SAC fibers after flexural test

hardened before the test, probably due to poor sealing of the ends of SAC fibers. The regaining of stiffness in the second reloading cycle is less significant. This is probably due to exhaustion of available sealing agent in the first damage/healing cycle.

There was not much difference between the re-healing behavior of the PSS–ECC systems using materials M1 and M2. A significant change of stiffness was found in S-M1-4, about 1.4 for the first reloading and 1.0 for the second reloading. This may be the result of a larger amount of sealing agent in the PSS–ECC system.

*Figure 17* shows a cut section of S-M1-4 after testing. The hollow glass fiber is broken at the location where the ECC crack crosses the fiber. This is further evidence of the sensing mechanism of the PSS–ECC system. Unfortunately, the crack shown in the picture does not appear to be sealed. It is possible that other cracks not shown in the picture ruptured the glass fiber first, and the sealing agent has been released into those regions. The crack shown in *Figure 17* presumably formed after the sealing agent had been released. The thin layer of hardened residual sealing agent on part of the inside glass fiber surface supports this hypothesis. This observation, together with the regained stiffness of this specimen, strongly supports the PSS–ECC concept. The self-healing effect could not have been achieved without the sensing and actuation mechanisms described.

## CONCLUSIONS

The feasibility of a PSS–ECC has been investigated via conceptual design, preliminary embodiment and experimental tests. The sensing action of overloading by ECC matrix cracking, and actuation of chemical release from hollow glass fibers embedded in an ECC by glass fiber breakage, were confirmed by direct observation of the sensing and actuation mechanisms in small specimens of a model PSS–ECC system tested *in situ* in an ESEM. The re-healing effect is validated by regaining of flexural stiffness in beams reloaded after an initial cycle of loading to beyond first cracking followed by unloading. Together, these experiments support the concept and viability of the self-healing passive smartness in the PSS–ECC.

While the potential of PSS–ECC is clarified in these laboratory studies, there remain issues which require further investigation before this material can be applied in the field. For example, further research and development are needed for effective filling and placing of the hollow glass fibers in large-scale applications. In addition, the shelf-life and economics of the chemical sealant need to be analyzed for practical applications. Finally, the sealing effectiveness of PSS–ECC after damage remains to be investigated in a future study. Even so, it can be concluded that a foundation for detailed development of the proposed PSS–ECC system has been established.

## ACKNOWLEDGEMENTS

The research described in this paper was supported by a grant from the National Science Foundation (BCS 9202097) and from the National Research Council (SHRP-91-ID036) to the University of Michigan.

## REFERENCES


1. Rogers, C.A., Intelligent materials. *Scientific American*, 1995, **273**, 154–157.
2. Li, V.C. Engineered cementitious composites—a tailored composite through micromechanical modeling. *Fiber Reinforced Concrete*: *Present and the Future* (Eds N. Banthia, A. Bentur and A. Mufti). Canadian Society of Civil Engineers, Montreal, Sept. 1998, pp. 64–97.
3. Dry, C.M., Smart multiphase composite materials which repair themselves by a release of liquids which become solids. *Proc. SPIE*, 1994, **2189**, 62–70.
4. Li, V.C. and Leung, C.K.Y., Steady state and multiple cracking of short random fiber composites. *ASCE J. Engineering Mechanics*, 1992, **118**(11), 2246–2264.
5. Li, V.C., From micromechanics to structural engineering—the design of cementitious composites for civil engineering application. *JSCE J. Struct. Mechanics and Earthquake Engineering*, 1993, **10**(2), 37–48.